Molecular Crystals and Liquid Crystals Science and Technology. Section A. Molecular Crystals and Liquid Crystals

Publication details, including instructions for authors and subscription information:
http://www.tandfonline.com/loi/gmcl19

Methods for Determination of Solubility Limits of Polymer-Dispersed Liquid Crystals

George W. Smith [a] & Nuno A. Vaz [a]

[a] Physics Department, GM Research, Warren, Michigan, 48090-9055

Version of record first published: 24 Sep 2006.

To cite this article: George W. Smith & Nuno A. Vaz (1993): Methods for Determination of Solubility Limits of Polymer-Dispersed Liquid Crystals, Molecular Crystals and Liquid Crystals Science and Technology. Section A. Molecular Crystals and Liquid Crystals, 237:1, 243-269

To link to this article: http://dx.doi.org/10.1080/10587259308030140

Mol. Cryst. Liq. Cryst., 1993, Vol. 237, pp. 243–269
Reprints available directly from the publisher
Photocopying permitted by license only

Printed in the United States of America

Methods for Determination of Solubility Limits of Polymer-Dispersed Liquid Crystals

GEORGE W. SMITH and NUNO A. VAZ

Physics Department, GM Research, Warren, Michigan 48090-9055

(Received October 1, 1992; in final form January 1, 1993)

Measurement of the solubility limit, A, of a liquid crystal (LC) in a polymer matrix is an important consideration in optimizing polymer-dispersed liquid crystal (PDLC) films for a variety of light-control applications. By reducing A, we can improve the efficiency of LC usage. We describe four methods—differential scanning calorimetry (DSC), threshold for light scattering (TLS), refractive index (RI) measurement, and scanning electron microscopy (SEM)—for determining A-values. We discuss the advantages and drawbacks of the various methods and present results to illustrate their use. Solubility limits can take on a wide range of values depending on the PDLC components, their cure temperatures, and the measurement temperature. For example, DSC measurements show that solubility increases with increasing measurement temperature. Also, thermally cured PDLCs studied so far have tended to have lower A-values than UV-cured ones. For thermally cured systems, A-values ranged from 8 to 36 volume percent; for UV-cured PDLCs, the range was broader: 9 to 53 volume percent. An important goal of future research would be the development of liquid crystal/polymer combinations for which phase separation is maximized (low A-values).

Keywords: polymer-dispersed liquid crystals, PDLCs, liquid crystals, solubilities, mixtures, polymer/liquid crystal mixtures

INTRODUCTION

Polymer-dispersed liquid crystals (PDLC) films, dispersions of micron-sized droplets of liquid crystal (LC) in a polymer matrix, have considerable potential for several applications, including displays and privacy windows. An important goal of current research is to minimize the amount of LC required for their fabrication. This could be achieved if most of the LC were entrapped in the microdroplets rather than dissolved in the polymer matrix. Therefore, it is important to use a LC/polymer matrix combination for which A, the liquid crystal solubility limit in the matrix, is low. A low value of A results in an enhanced degree of phase separation of LC from the cured matrix, thus helping to maximize α, the fraction of liquid crystal in the droplets. Knowledge of A makes it possible to calculate α using a previously reported mathematical model.[1,2]

It is obviously important to develop accurate methods to measure A. In this paper we describe several techniques which allow us to determine A (and hence α). These methods include differential scanning calorimetry (DSC), threshold for light scattering (TLS), refractive index (RI), and scanning electron microscopy

(SEM). The DSC method has been reported previously,[2] but additional data are presented here.

In the next three sections, we shall i) describe our experimental techniques, ii) present results of several studies, and iii) discuss the implications of these studies for efficient use of liquid crystals.

EXPERIMENT

Sample Preparation

The PDLCs were all prepared using thermoset polymer matrices and single- or multi-component liquid crystals. Specific materials will be discussed in the Results section. Cross-linking of the polymer matrices was achieved using either thermal or UV-cure techniques described previously.[1-8] In some cases the influence of cure temperature on PDLC parameters was also determined.

Samples for Calorimetry. Epoxy-based PDLCs were thermally cured prior to DSC studies[2]; all other systems were cured directly in the calorimeter as discussed elsewhere.[1,5,8] Initially the components (liquid crystal and polymer precursors) were mixed outside the calorimeter, micropipetted into sample pans, weighed, and then introduced into the DSC sample chamber. Cure was then carried out either thermally[1,4,5] or by ultraviolet irradiation (UV cure).[3,8] The experimental technique for UV cure of samples was more complicated than that for thermal cure since it was necessary to use special sample pans and to introduce the UV into the calorimeter by means of a light pipe.[8] Cure temperatures ranged from 313 K to 400 K (40°C to 127°C) for thermally-cured systems and from 300 K to 400 K (27°C to 127°C) for UV-cured PDLCs.

Samples for Threshold for Light Scattering Studies. For our TLS work we prepared a batch of samples containing 5 to 25 volume percent LC dissolved in monomer/oligomer mixtures. The components for a given sample were stirred together at about 333 K (60°C) to insure complete homogenization. At least five droplets of each sample were placed at intervals on a glass plate coated with a transparent conductor (indium tin oxide [ITO]). The glass plate was maintained at about 333 K in order to avoid unwanted phase separation prior to UV cure. A small number of 20 μm spacer particles[9] was then dispersed over the surface and a second (preheated) glass plate was placed (conducting side down) on top of the droplets. A low pressure was applied to spread the droplets into five (or more) small spatially separated films while maintaining the desired 20 μm spacing.

The batch of sample plates was then transported by a conveyor system into a cure chamber where the samples were all cured simultaneously using a Fusion Systems model F-460 UV-light apparatus capable of delivering 300 W/in of UV irradiation.[10] The temperature in the chamber was maintained at 318 K (45°C) during the cure process. With the conveyor moving at 8.6 ft/min, the samples were cured after one pass under the focal line of the UV radiation. The use of five small films for each sample helped to minimize error due temperature or UV non-

uniformities. Simultaneous cure of the batches insured a high degree of uniformity in the curing conditions for all samples.[11]

Samples for Refractive Index Studies. Refractive indices were measured using a Jelley-Leitz refractometer[12] and previously described techniques.[13,14] Samples were prepared as follows: Small amounts of LC, monomers, and oligomers were mixed at a temperature sufficiently above room temperature to insure complete homogenization and placed in the gap between the optical prism of the refractometer and a thin optical flat. The assembly was then placed in a Fusion Systems Model Super 6 UV-curing apparatus capable of delivering 200 W/in of UV irradiation.[10] Cure was carried out under conditions similar to those for TLS. The only major difference was that no special care was taken to control the sample thickness. The Jelley prism with the cured mixture was mounted in the hot stage of the refractometer and the refractive index measured as a function of temperature.

Samples for Scanning Electron Microscopy. Samples for SEM analysis of microstructural features were prepared using thermal cure techniques previously described[3,6] at temperatures ranging from 298 K to 373 K (25°C to 100°C). Each cured sample was cross-sectioned to expose its interior. The liquid crystal thus exposed was removed under vacuum and the sample coated (at temperatures a few degrees above ambient) with a thin layer of gold-palladium alloy. Occasionally we found that some LC would migrate from the sample interior and destroy the metal coating. In such cases better results could be obtained by washing the exposed surface of the sample with a solvent before vacuum treatment. Finally, the sample was mounted on the carousel of a ISI SEM instrument[15] and examined using a magnification of about 4000 times.

Experimental Techniques

Calorimetry. The differential scanning calorimeter used in these studies was a Perkin-Elmer DSC2 described previously.[1,3–6,16] When sample cure was carried out in the calorimeter, the instrument was operated isothermally. Cure energetics/kinetics and phase behavior studies have been previously studied for several of the PDLC systems.[1,5,6,8,17]

In order to determine the solubility limit of the PDLCs, we operated the instrument in its temperature scanning mode.[5] In this mode the sample temperature was programmed linearly over the range of interest while the sample's heat absorption rate, dQ/dt, was recorded (Figure 1). The resulting thermal spectra (plots of dQ/dt as a function of temperature) enabled us to determine temperatures of phase transitions and their associated enthalpies or specific heat changes using the instrument's thermal analysis data station.[1,5,8,16] Sample temperatures as low as 190 K (−83°C) were attained by use of a Perkin-Elmer Intracooler II[16] refrigeration system. Program (scanning) rates of 10 K/min or 20 K/min were used.

Two quantities are of particular importance in determining A from DSC measurements. The first of these is ΔC_{LC}, the incremental increase in specific heat (per unit mass) at $T_{g,LC}$, the glass transition temperature of "free" liquid crystal (i.e., LC not dissolved in the polymer matrix).[2] For sufficiently low LC concentrations (usually $\leq 50\%$) this free liquid crystal is all contained in the PDLC microdroplets.

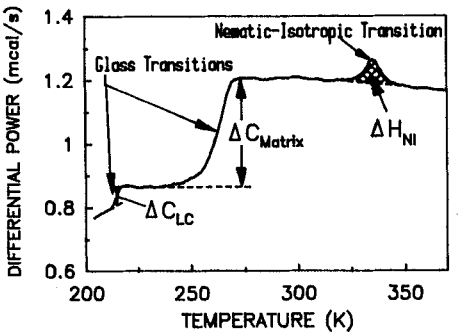

FIGURE 1 Typical differential scanning calorimetry (DSC) thermal scan for a polymer-dispersed liquid crystal (PDLC). Three calorimetric quantities are indicated: ΔC_{LC}, the specific heat increment associated with the glass transition due to liquid crystal in the microdroplets; ΔC_{Matrix}, the specific heat increment due to the polymer matrix glass transition; and ΔH_{NI}, the nematic-isotropic transition enthalpy.

(For higher concentrations some, or all, of the free LC may form large "puddles" or even become a continuous phase.) For sufficiently low LC concentrations, all the liquid crystal is dissolved in the polymer matrix and $\Delta C_{LC} \rightarrow 0$. The second parameter of interest is ΔH_{NI}, the change in enthalpy (per unit mass) at the nematic-isotropic transition temperature, T_{NI}. Like ΔC_{LC}, ΔH_{NI} is due to LC in the microdroplets,[2] and the same considerations regarding LC concentration apply to ΔH_{NI} as well as to ΔC_{LC}.

These two calorimetric quantities are illustrated in the DSC thermogram of Figure 1. ΔH_{NI} is determined by integrating the area of the NI peak above a properly selected baseline, ΔC_{LC} by measuring the magnitude of the increase in specific heat between two baselines extrapolated from well below and well above the glass transition region.[2] A third quantity derivable from the DSC thermogram is the specific heat increment, ΔC_{Matrix}, at the matrix glass transition temperature, $\Delta T_{g,Matrix}$ (see Figure 1). This parameter is of little interest in determining the solubility limit, A.

The theoretical basis for determining A from ΔC_{LC} and ΔH_{NI} is straightforward and has been derived elsewhere.[1,2] The relation between the calorimetric quantities and A is

$$P = (X - A)/(100 - A) \qquad (X \geq A), \tag{1}$$

where P is equal to either:

$\Delta C_{LC}(X)/\Delta C_{LC}(LC)$, the ratio of the LC specific heat increment for a PDLC containing X percent LC to that for the pure LC,

or to:

$\Delta H_{NI}(X)/\Delta H_{NI}(LC)$, the ratio of the nematic-isotropic transition enthalpy for a PDLC containing X percent LC to that for the pure liquid crystal.

It should be emphasized that Equation 1 is exact only if X is expressed as a

weight percent; for X as a volume percent, the expression is approximate.[1,2] (However, the approximation is very good when the LC and polymer precursor densities are nearly equal, as is often the case.[1])

A is determined by fitting concentration-dependent measurements of ΔC_{LC} and ΔH_{NI} to Equation 1. Then α, the fraction of LC contained in the microdroplets, can be calculated from[1,2]

$$\begin{aligned} \alpha &= 0 && (X < A) \\ \alpha &= (100/X)(X - A)/(100 - A) && (X \geq A) \end{aligned} \tag{2}$$

Equation 2 is exact for X and A expressed as either weight or volume percentages.[1,2] Of course, Equation 2 is applicable no matter how the A-value is determined, whether from DSC, TLS, RI, or SEM.

Threshold for Light Scattering (TLS). Light scattering by PDLC films results from refractive index mismatches at the interfaces between the polymer matrix and the LC droplets. Thus, the existence of light scattering (LS) is a clear fingerprint for the presence of LC microdroplets. By preparing a batch of PDLC samples with various liquid crystal concentrations, X, and visually inspecting them for signs of light scattering, we could set upper and lower bounds on the solubility limit of the

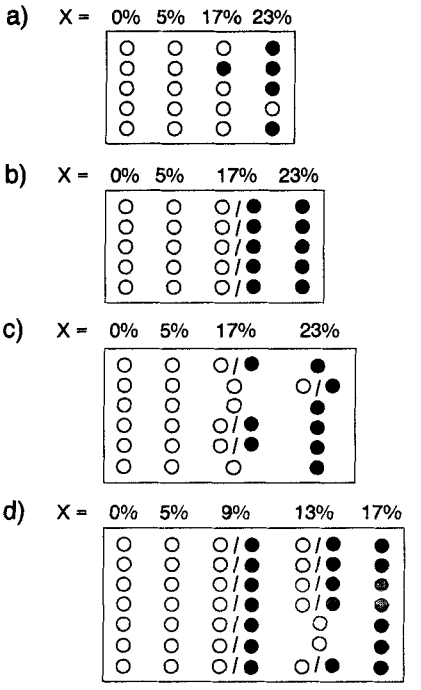

FIGURE 2 Results of light scattering tests on four different BL009/polymer UV-cured mixtures. For each polymer 4 or 5 sets of samples were prepared with differing LC concentrations, X, each set containing several (5 to 7) identical samples. Open circles (closed circles) indicate non-scattering (scattering) samples. a) BL009/NOA65, $A = 20 \pm 3\%$; b) BL009/NR1, $A = 17 \pm 3\%$; c) BL009/P6008A, $A = 17 \pm 3\%$; d) BL009/P6008B, $A = 11 \pm 3\%$.

LC. The TLS method is illustrated by the schematic sample arrays shown in Figure 2.

Two cautionary notes are in order:

1. The upper and lower bounds on A are the lowest concentration for which LS is observed and the concentration just below that. Thus, the precision of the method is determined by the size of the incremental increases in LC concentration used in preparing the sample set. In our experiments we increased X in steps of 5%, which limits the precision of our determinations to about 2.5%.
2. Even though LS indicates the presence of droplets, its absence does not mean that droplets are not present. There are two reasons why this should be so. A PDLC film may remain transparent after droplet formation if there is only a small index mismatch between the LC and polymer matrix (see References 18–22 for a discussion of different ways this situation can arise). Alternatively, the size and number density of droplets may be such that light scattering is minimal. We believe that for our systems only the latter case is a factor. This being the case, the solubility limit determined from TLS should be, at worst, an overestimate of the true value of A. Accordingly, we define the value of the solubility limit determined from TLS to be the lower bound discussed above.

Refractive Index. Measurements of the refractive index of mixtures of LC, monomers, and oligomers cured under identical conditions reveal the influence of the liquid crystal on the optical properties of the polymer matrix. Indeed, one might expect that, when the concentration of LC approaches the solubility limit, the mechanisms driving the phase separation process would lead to appreciable changes in the optical properties of the system. In particular, the refractive index could depart from ideal dependence on materials concentrations. In order to probe for such effects, we investigated the temperature dependence of the refractive indices of several starting materials and their mixtures.

Index measurements were carried out at temperatures from ~300 K to ~400 K (~30°C to ~130°C). Data were taken for both increasing and decreasing temperature, and the results were averaged. As is well known,[13] the refractive index, $n(T)$, varies linearly with temperature:

$$n(T) = n_{T0} + (dn/dT)_{T0} \times (T - T_0), \tag{3}$$

where T_0 is taken to be 298 K (25°C). From a linear regression, the two constants of Equation 3 were determined for several liquid crystals, pure polymer matrices, and their cured mixtures. It was felt that the values of n and dn/dT might undergo meaningful changes as the LC concentration approached the solubility limit. The reasoning behind this belief is as follows: As pointed out by Vaz and Montgomery,[13] the refractive index of a mixture varies linearly with the volumetric concentration of one of the components only if the mixture is ideal. For LC concentrations close to A, we expected the mixture to depart from ideality. That being the case, the measured index for the mixture and/or its temperature dependence should differ significantly from the value determined using the linear model.

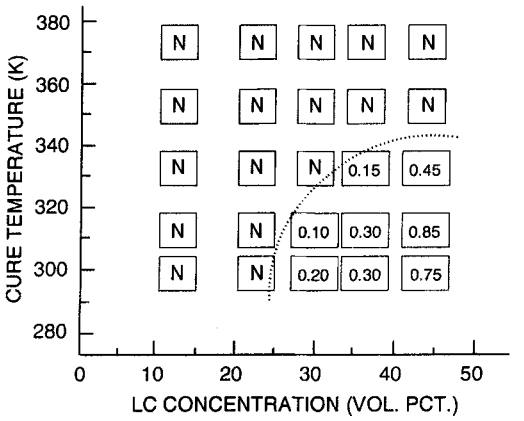

FIGURE 3 "Phase diagram" for epoxy-based films. The entries identify the composition and the cure temperature of each sample, the letter "*N*" indicates that a sample did not scatter light (i.e., did not contain microdroplets). The numbers are averaged droplet diameters (μm) for those samples which did scatter light.

SEM Analysis. Scanning electron microscope (SEM) photomicrographs of PDLCs can be used to determine the volumetric number density, n_V, of LC microdroplets as well as the droplet diameter, D. Examination of micrographs of samples with various LC concentrations cured at several temperatures, allowed us to determine, for each cure temperature (T_{cure}), that concentration for which n_V approached zero (i.e., the solubility limit). The results of such an examination are shown in the "phase diagram" of Figure 3. The entries in the figure identify the LC concentration of T_{cure} value of each sample; the "*N*" symbols indicate that a sample does not scatter light. For those samples which do scatter light, the mean microdroplet diameter is given. In the phase diagram a boundary curve separates homogeneous samples (i.e., those with $n_V = 0$) from those containing droplets. Obviously, this boundary curve defines the solubility limit for each cure temperature. This method of obtaining A can be made relatively precise (see Results section).

RESULTS

Calorimetry

Thermally-Cured Epoxy-Based Systems. Results for three types of thermally cured epoxy-based PDLCs have been reported previously.[2] The systems were all prepared at Kent State University,[23] two using a two-part Bostik epoxy[24] and two different single component liquid crystals (5CB and 7CB)[25]; the third used a three-part index-matched epoxy and E7, a four component liquid crystal.[25] The previously reported solubility limits[2] were all weight percent values. For comparison with other results in this report, we have converted the A-values to volume percentages in Table I. Since the densities of the two epoxies are considerably larger than for the liquid crystals, the volumetric A-values are 11 to 14% larger than the corre-

TABLE I

A-Values for thermally-cured epoxy-based PDLCs (from DSC)

Liquid crystal	Matrix	Cure temperature	A (vol. pct.) from ΔC_{LC} [f]	A (vol. pct.) from ΔH_{NI} [g]
5CB[a]	Bostik[d]	313 K (40°C)	15.7	21.0
7CB[b]	Bostik[d]	313 K (40°C)	10.3	15.4
E7[c]	3-part[e]	323 K (50°C)	16.0	8.1
		343 K (70°C)	12.9	10.5
		363 K (90°C)	15.4	16.8

[a]4-*n*-pentyl-4′-cyanobiphenyl[25]; density $\rho = 1.023$ g/cm^3.
[b]4-*n*-heptyl-4′-cyanobiphenyl[25]; $\rho = 1.010$ g/cm^3.
[c]4-component LC[25]; $\rho = 1.028$ g/cm^3.
[d]2-part epoxy[24]; $\rho = 1.17$ g/cm^3.
[e]3-part epoxy[2]; $\rho = 1.10$ g/cm^3.
[f]Temperatures for ΔC_{LC} results: 5CB/Bostik and 7CB/Bostik: 205 K (−68°C); E7/3-part: 215 K (−58°C).
[g]Temperatures for ΔH_{NI} results: 5CB/Bostik: 314 K (41°C); 7CB/Bostik: 317 K (44°C); and E7/3-part: 336 K (63°C).

sponding weight *A*-values for the Bostik-based systems and 6% larger for the PDLC based on the three-part epoxy.

Table I shows that, for the single component LCs (5CB and 7CB), ΔC_{LC} yields lower values of A than does ΔH_{NI}. This result is due to the lower LC solubility in the matrix at the LC glass transition temperature (which is about 100 K lower than T_{NI}). The large difference between A-values from ΔC_{LC} and ΔH_{NI} for the E7/epoxy sample cured at 323 K (50°C) is not understood. Factors contributing to the discrepancy may be preferential solution in the polymer matrix of low molecular weight liquid crystal components and possibly incomplete cure of the matrix for high LC concentrations. In addition, it should be kept in mind that the experimental scatter in measured values of ΔC_{LC} is somewhat lower than for ΔH_{NI}. The larger error in ΔH_{NI} perhaps results from the difficulty in obtaining a correct baseline for integration of the NI peak.

Thermally-Cured Polyurethane-Based System. Calorimetric studies of thermally-cured PDLCs based on a polyurethane matrix have also been reported.[1] The liquid crystal in this case was ROTN404, a six-component mixture with a wide nematic temperature range.[26] Unfortunately, only ΔH_{NI} values were measured for these PDLCs; DSC measurements were not extended to low enough temperatures to include ΔC_{LC}. Nevertheless A-values for samples cured at two different temperatures were derived from best fits to the ΔH_{NI} data for LC concentrations ranging from 18 to 63 volume percent. For $T_{cure} = 375$ K (102°C), $A = 15.5$ volume percent; for $T_{cure} = 400$ K (127°C), $A = 16.8$ volume percent. The nematic-isotropic temperature of this system is quite sensitive to LC content[1]: as X increases from 18% to 63%, T_{NI} increases from ~325 K (62°C) to ~375 K (102°C). Consequently, the measurement temperature for which the A-values are characteristic must be taken to be some sort of average: 350 ± 25 K (77 ± 25°C).

UV-Cured Thiol-ene-Based Systems. Prior DSC investigations of ultraviolet-

cured PDLCs[3,6,8] have been directed toward optimization of cure conditions (i.e., UV intensity, cure temperature, etc.) rather than toward solubility considerations. Therefore, concentration-dependent calorimetric studies to determine A-values for UV-cured systems have not been previously reported. In this section we describe such an investigation of two UV-cured PDLCs.

The polymer matrix for both PDLC systems was Norland UV-curable optical adhesive 65 (abbreviated NOA65),[27] use of which has been previously discussed.[3,8,28] The liquid crystals were each multi-component mixtures, ROTN404[26] (see above) and BL009.[25]

ROTN404/NOA65 PDLCs (with LC concentrations of 0, 20, 33, 50, and 67 volume percent) were prepared in the usual manner[8] and were UV-cured in the calorimeter at temperatures of 300, 325, 336, 350, and 375 K (27, 52, 63, 77, and 102°C). Cure temperatures of the BL009/NOA65 samples (with LC concentrations of 0, 50, and 67 volume percent) ranged from 300 K to 400 K (27°C to 127°C). For both sets of samples we expect a "reverse morphology"[29,30] for LC concentrations of 67%. Nevertheless we include data for this concentration because ΔC_{LC} and ΔH_{NI} for all values of X are relevant to a derivation of the solubility limit, even if the LC is a continuous phase.[2]

ROTN404/NOA65 system. The glass transition temperatures, T_g, of the LC in

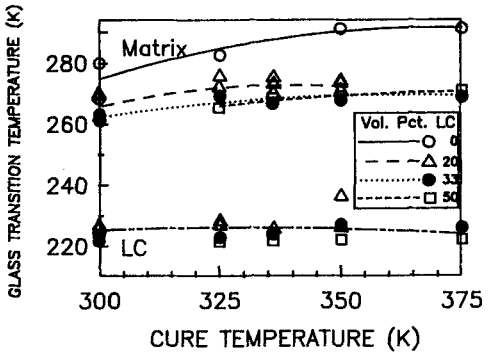

FIGURE 4 Glass transition temperature vs. cure temperature for ROTN404/NOA65 PDLCs.

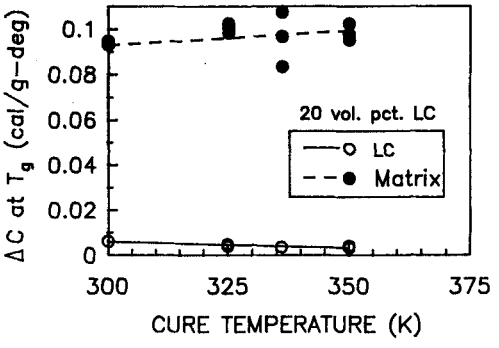

FIGURE 5 Specific heat increments, ΔC_{LC} and ΔC_{Matrix}, versus cure temperature for a ROTN404/NOA65 PDLC with a LC concentration of 20 volume percent.

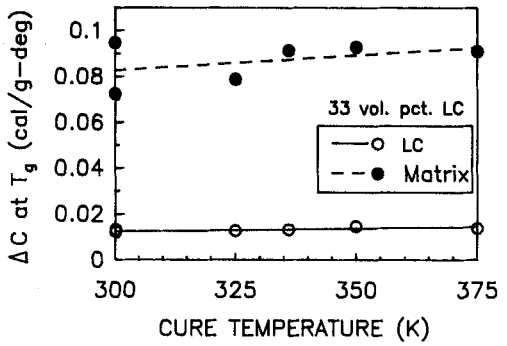

FIGURE 6 ΔC_{LC} and ΔC_{Matrix} versus cure temperature for a ROTN404/NOA65 PDLC with a LC concentration of 33 volume percent.

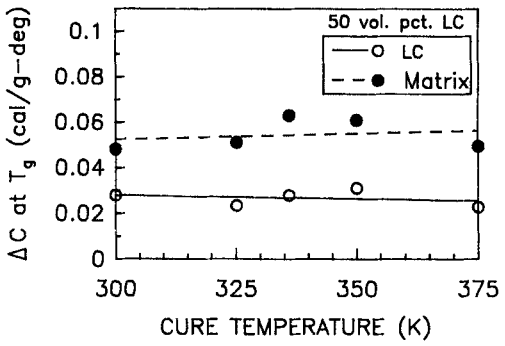

FIGURE 7 ΔC_{LC} and ΔC_{Matrix} versus cure temperature for a ROTN404/NOA65 PDLC with a LC concentration of 50 volume percent.

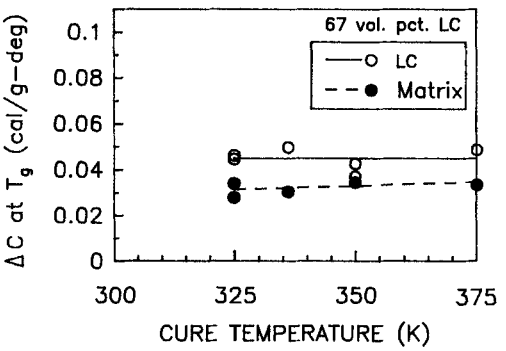

FIGURE 8 ΔC_{LC} and ΔC_{Matrix} versus cure temperature for a ROTN404/NOA65 PDLC with a LC concentration of 67 volume percent.

the droplets and of the polymer matrix are plotted as a function of cure temperature in Figure 4. As has been previously observed for both UV-cured[3] and thermally-cured[1] systems, the matrix T_g decreases with increasing LC concentration due to the plasticizing effect of the liquid crystal. In contrast, the glass transition tem-

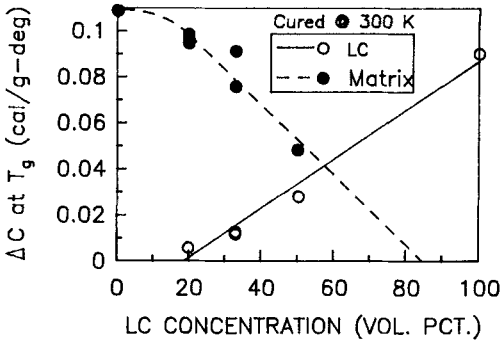

FIGURE 9 ΔC_{LC} and ΔC_{Matrix} versus LC concentration for a ROTN404/NOA65 polymer-dispersed liquid crystal cured at 300 K (27°C).

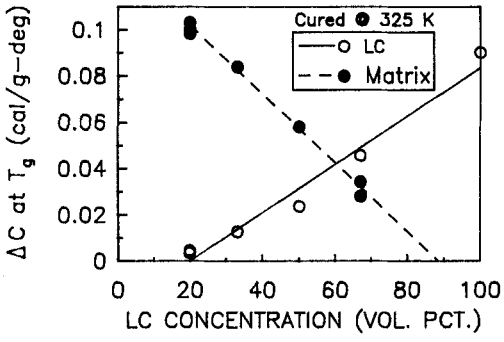

FIGURE 10 ΔC_{LC} and ΔC_{Matrix} versus LC concentration for a ROTN404/NOA65 polymer-dispersed liquid crystal cured at 325 K (52°C).

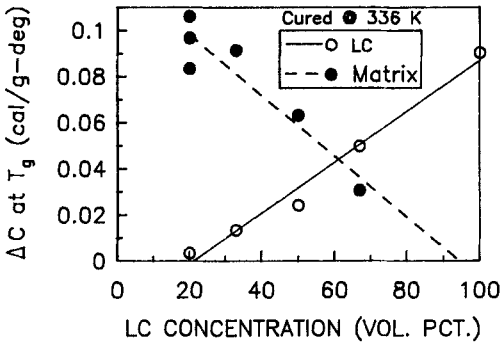

FIGURE 11 ΔC_{LC} and ΔC_{Matrix} versus LC concentration for a ROTN404/NOA65 polymer-dispersed liquid crystal cured at 336 K (63°C).

perature of the LC in the droplets does not depend strongly on either T_{cure} or LC concentration. The dependences of ΔC_{LC} and ΔC_{Matrix} on cure temperature are given in Figures 5–8. Although both quantities are fairly insensitive to T_{cure}, there is a strong dependence on LC concentration. This is seen more clearly in Figures 9–13, where ΔC_{LC} and ΔH_{NI} are plotted versus X for five cure temperatures.

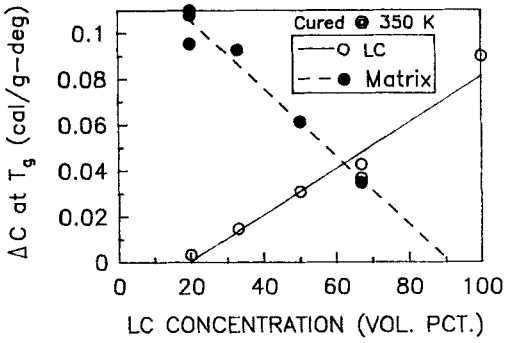

FIGURE 12 ΔC_{LC} and ΔC_{Matrix} versus LC concentration for a ROTN404/NOA65 polymer-dispersed liquid crystal cured at 350 K (77°C).

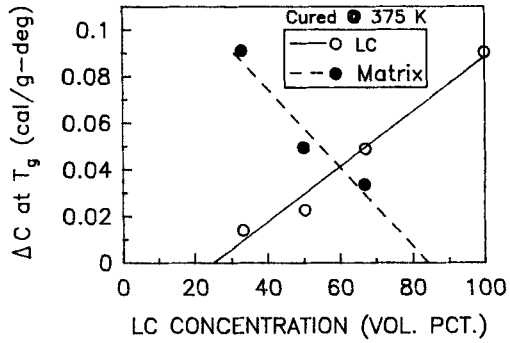

FIGURE 13 ΔC_{LC} and ΔC_{Matrix} versus LC concentration for a ROTN404/NOA65 polymer-dispersed liquid crystal cured at 375 K (102°C).

A-values were derived from linear regression fits to the plots of ΔC_{LC} vs. X and are listed in Table II and plotted in Figure 14 (along with A-values derived from ΔH_{NI}—see below). The measurement temperature for the A-values characteristic of ΔC_{LC} is, of course, low ($T_{g,LC} \simeq 225$ K).

In Figure 15 the dependence of the nematic-isotropic transition temperature on T_{cure} is plotted for $X = 50\%$ and 67%. Although LC glass transitions were observed for samples with $X = 20\%$ and 33% (see Figures 5 and 6), no nematic-isotropic transition peaks were detectable for any samples with these two concentrations. Apparently for temperatures on the order of T_{NI} and X-values of 20% and 33%, all the ROTN404 is dissolved in the NOA65. This conclusion is consistent with the fact that the A-value at T_{NI} is approximately 40% (Figure 14). For $X = 50\%$, T_{NI} increases with T_{cure}, but remains below the value for the pure LC (384 K). Such an increase in T_{NI} with cure temperature has been previously observed for both thermally-cured and UV-cured PDLCs.[5,6] T_{NI} for $X = 67\%$ is essentially independent of T_{cure}, perhaps as a result of the formation of a reverse morphology (with LC the continuous phase) for this high concentration.

Plots of ΔH_{NI} versus cure temperature for $X = 50\%$ and 67% are given in Figure 16. Although the scatter is large, for $X = 50\%$ there appears to be a maximum

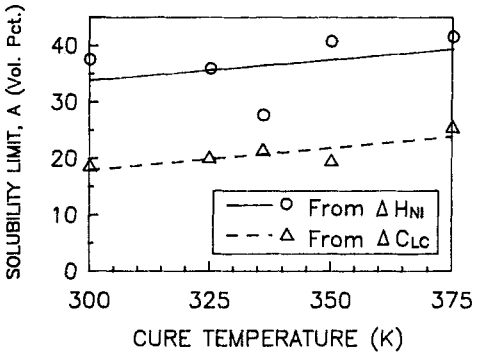

FIGURE 14 Solubility limits versus cure temperature for ROTN404/NOA65 PDLCs. A-values derived from ΔH_{NI} are substantially higher than those from ΔC_{LC}.

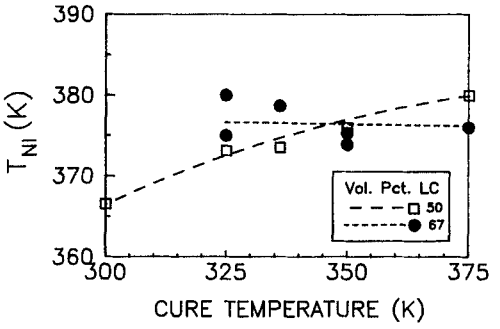

FIGURE 15 Nematic-isotropic transition temperature versus cure temperature for ROTN404/NOA65 PDLCs.

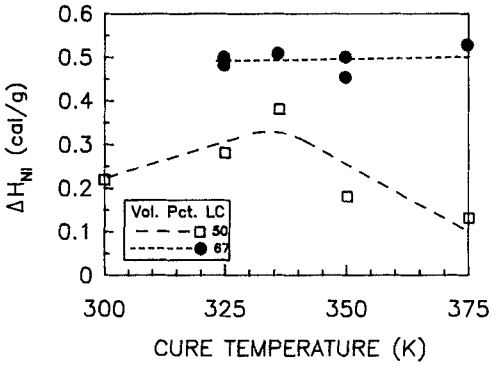

FIGURE 16 Nematic-isotropic transition enthalpy versus cure temperature for ROTN404/NOA65 PDLCs.

near 335 K (62°C). It has been previously shown[8] that, for a similar UV-cured PDLC, phase separation is greatest near this cure temperature, resulting in a maximum of ΔH_{NI}. For $X = 67\%$, ΔH_{NI} is constant, suggesting that, for the reverse morphology, the fraction of LC dissolved in the matrix does not change with cure temperature. The dependence of ΔH_{NI} on X is shown in Figure 17 for five cure

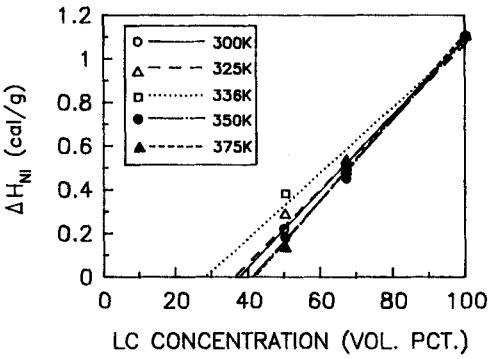

FIGURE 17 Nematic-isotropic transition enthalpy versus LC concentration for ROTN404/NOA65 PDLCs cured at five different temperatures.

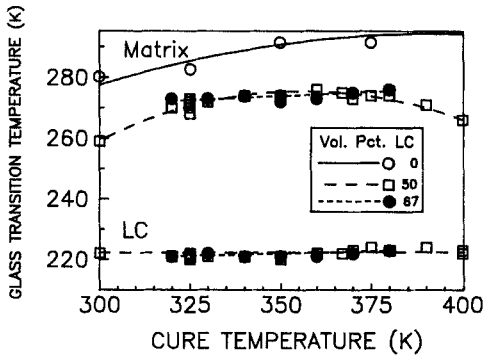

FIGURE 18 Glass transition temperature vs. cure temperature for BL009/NOA65 PDLCs.

temperatures. Linear regressions to the data of this figure yielded the A-values shown in the upper curve of Figure 14 and in Table II. Since the dependence of T_{NI} on LC concentration (Figure 15) is considerably less than that for the thermally-cured ROTN404/polyurethane system,[1] the spread in the mean temperature characteristic of the A-values is smaller: ~373 ± 7 K (~100 ± 7°C). Because data at only three concentrations were available for each $\Delta H_{NI} - X$ curve, the uncertainties in the A-values derived from the transition enthalpy are rather large for this system. (As mentioned in the previous paragraph, the lack of a NI peak for X = 20% and 33% is due to the greater solubility of the LC in the matrix at T_{NI}, a fact which is not altogether surprising since T_{NI} is some 150 K higher than $T_{g,LC}$.)

BL009/NOA65 system. The glass transition temperatures for this PDLC are plotted in Figure 18. As was the case for ROTN404/NOA65 (Figure 4), $T_{g,LC}$ is fairly insensitive to both LC concentration and T_{cure}. The temperature dependences of $T_{g,Matrix}$ for the two systems are similar, but an increase in X appears to have a smaller effect on $T_{g,Matrix}$ for the BL009 compound than on that for the ROTN404 PDLC. The dependences of ΔC_{LC} and ΔC_{Matrix} on T_{cure} are given in Figure 19. A comparison with Figures 7 and 8 shows that the behavior for the BL009 system is similar to that for the ROTN404 one; that is, for X = 50% $\Delta C_{LC} < \Delta C_{Matrix}$, and for X = 67% $\Delta C_{LC} > \Delta C_{Matrix}$. The dependence of the specific heat increments

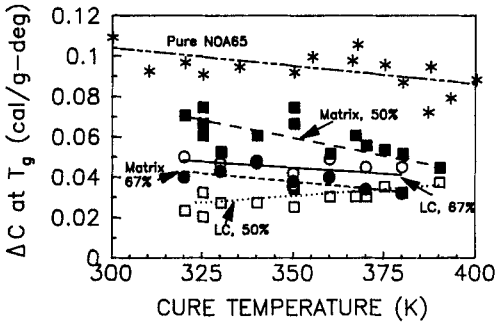

FIGURE 19 Specific heat increments, ΔC_{LC} and ΔC_{Matrix}, versus cure temperature for BL009/NOA65 PDLCs with LC concentrations of 50 and 67 volume percent.

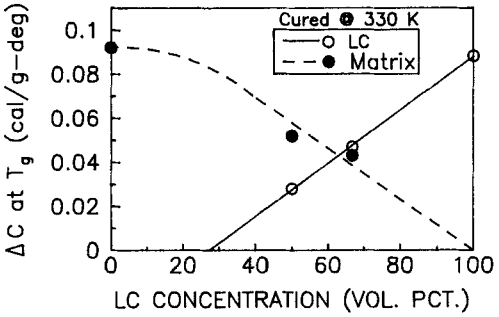

FIGURE 20 Specific heat increments, ΔC_{LC} and ΔC_{Matrix}, versus LC concentration for BL009/NOA65 PDLCs cured at 330 K (57°C).

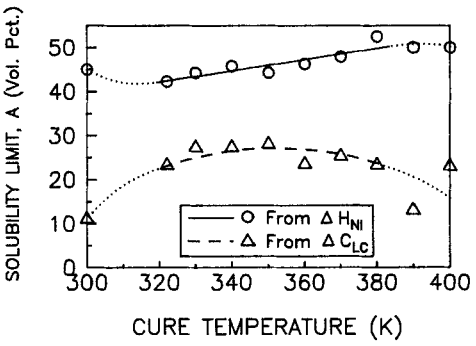

FIGURE 21 Solubility limits versus cure temperature for BL009/NOA65 PDLCs. A-values derived from ΔH_{NI} are substantially higher than those from ΔC_{LC}.

on LC concentrations does not change greatly with cure temperature. Typical behavior, for T_{cure} = 330 K (57°C), is shown in Figure 20. A-values derived from plots of ΔC_{LC} vs. X are given in the lower curve of Figure 21 and in Table II. The measurement temperature for these values is, as before, low ($T_{g,LC} \simeq 222$ K).

The dependences of T_{NI} on T_{cure} for two LC concentrations are plotted in Figure 22. The curve for 50% is reminiscent of that for ROTN404/NOA65 (Figure 15).

TABLE II

A-Values for UV-cured PDLCs (from DSC)

Cure temperature	A (from ΔC_{LC})[a,b] (vol. pct.)	A (from ΔH_{NI})[c,d] (vol. pct.)
ROTN404/NOA65		
300 K (27°C)	18.6	37.5
325 K (52°C)	19.9	35.9
336 K (63°C)	21.3	27.7
350 K (77°C)	19.4	40.9
375 K (102°C)	25.3	41.6
BL009/NOA65		
322 K (49°C)	23.2	42.3
330 K (57°C)	27.3	44.3
340 K (67°C)	27.3	45.8
350 K (77°C)	28.0	44.3
360 K (87°C)	23.5	46.3
370 K (97°C)	25.3	47.9
380 K (107°C)	23.3	52.5

[a]Measurement temperatures for ΔC_{LC} results
For ROTN404/NOA65: ~225 K (−48°C) (see Figure 4)
For BL009/NOA65: ~222 K (−45°C) (see Figure 18).
[b]Number of LC concentrations available for fits to ΔC_{LC} for ROTN404/NOA65: 4 or 5; for BL009/NOA65: 3.
[c]Measurement temperatures for ΔH_{NI} results
For ROTN404/NOA65: ~366 K (93°C) to ~380 K (107°C) (Figure 15)
For BL009/NOA65: ~367 K (94°C) to ~390 K (117°C) (Figure 22).
[d]Number of LC concentrations available for fits to ΔH_{NI} for ROTN404/NOA65: 3 (except for T_{cure} = 300 K for which n_{LC} = 2); for BL009/NOA65: 3.

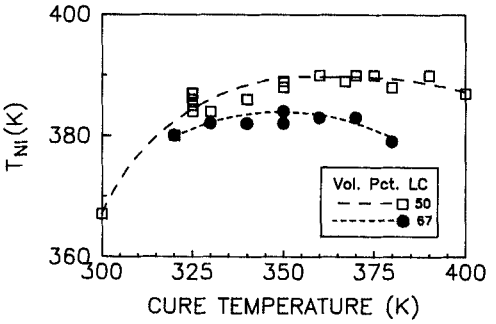

FIGURE 22 Nematic-isotropic transition temperature versus cure temperature for BL009/NOA65 PDLCs.

However, for $T_{cure} \sim 375$ K, T_{NI} slightly exceeds the value for pure BL009 (386 K), perhaps due to preferential solution of lighter LC components in the matrix. The depression of the T_{NI} curve for $X = 67\%$ may be due to impurities. Plots of ΔH_{NI} vs. cure temperature are given in Figure 23 for the same two LC concentrations. It was not possible to determine whether a maximum was present for $X = 50\%$ due to phase separation of the LC from the matrix precursor which takes place prior to cure at temperatures below 320 K. However, there is a slight indi-

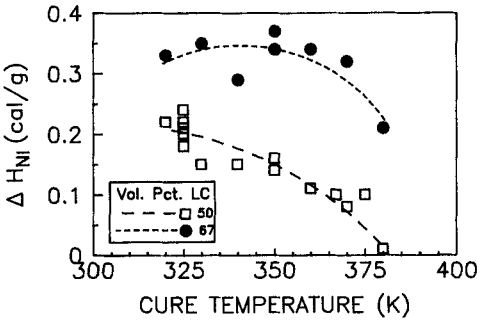

FIGURE 23 Nematic-isotropic transition enthalpy versus cure temperature for BL009/NOA65 PDLCs.

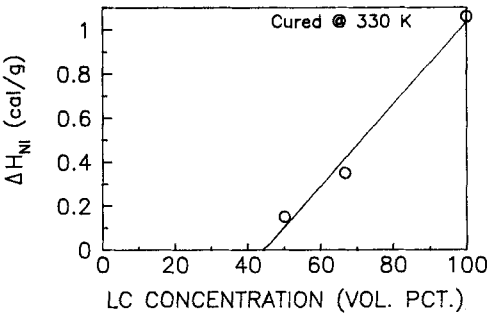

FIGURE 24 Nematic-isotropic transition enthalpy versus LC concentration for BL009/NOA65 PDLCs cured at 330 K (57°C).

cation of a maximum in the 67% curve. The rapid decrease in ΔH_{NI} above 350 K for both curves shows that much of the LC remains dissolved in the matrix at elevated cure temperatures. A typical plot of ΔH_{NI} vs. LC concentration is shown in Figure 24. Solubility limits derived from such plots are given in Table II and Figure 21 (upper curve). The A-values from both ΔC_{LC} and ΔH_{NI} for T_{cure} = 300 K (27°C) are suspect because of the pre-cure phase separation mentioned above. Also the A-values for cure temperatures of 390 K and 400 K (117 and 127°C) are subject to increased error due to the fact that data for only two concentrations were obtained for those temperatures. If we discard the suspect A-values, the curves of Figure 21 are similar to those of Figure 14. T_{NI} for cure temperatures from 322 K to 380 K lies between 380 K and 390 K (Figure 22), so that the measurement temperature for the corresponding A-values derived from ΔH_{NI} is taken to be slightly greater than 380 K.

Solubility Limits for Both Systems (cf. Figures 14 and 21 and Table II). A-values derived from ΔC_{LC} show little scatter and change slightly with T_{cure}. On the other hand, results from ΔH_{NI} are considerably higher than those from the specific heat increment. As mentioned above, this difference is due (at least in part) to the higher solubility of LC in the matrix at T_{NI}. The A-values for these two UV-cured systems are more sensitive to the measurement temperature than are those for the thermally cured PDLCs. Analysis of a limited amount of data for another UV-cured system (E7/NOA65) yielded an A-value at T_{NI} comparable to that for those two systems.[17]

Threshold for Light Scattering

Solubility limits for four different systems were determined by the TLS method. As explained above, the A-values were taken to be the minimum LC concentrations necessary to produce a PDLC film capable of scattering light.

The same liquid crystal, BL009,[25] was used in all four systems. This LC is a mixture consisting mostly of cyanobiphenyl and terphenyl materials. Four different UV-curable pre-polymer matrices were used: NOA65, a thiol-ene optical adhesive[27]; NR1, a thiol-ene formulation based on NOA65[31]; and P6008A[32] and P6008B,[33] two diurethane acrylate mixtures, the second of which contains an accelerator. Samples for each system were prepared using LC concentrations of 0, 9, 17, and 23 volume percent for the first three prepolymers and 0, 5, 9, 13, and 17 volume percent for the last one.

The results for the four systems are given in Figure 2. As can be seen, the A-values for the first three systems are on the order of 17 volume percent, whereas that for the fourth one is roughly 9 volume percent. The fact that A is low for the fourth system suggests that rapid cure (due to the accelerator) may play an important role in determining the degree of phase separation. Solubility limits were measured at room temperature (~295 K).

Refractive Index

In our refractive index studies we investigated two systems involving two different LCs and one pre-polymer resin: ROTN404/NOA65 and BL009/NOA65. The materials have been described in the previous sections. The refractive indices of the polymer matrix and of the PDLC mixtures were measured after UV-cure (as explained above) and are plotted in Figures 25 and 26. The ordinary and extraordinary indices, n_0 and n_e, of the pure liquid crystals were also measured using the methods of Reference 13.

For a sample with LC concentration less than A, all the liquid crystal is dissolved in the polymer matrix. In order to calculate the refractive index of such a sample it is necessary to take account of both matrix and LC indices. A simple additivity

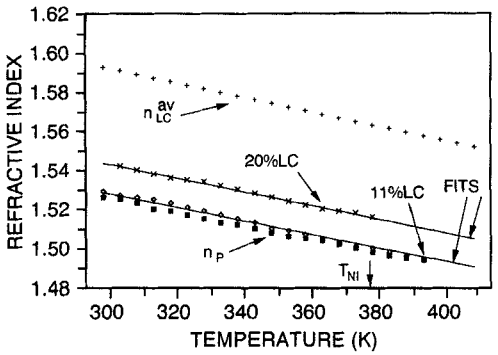

FIGURE 25 Temperature dependence of the refractive indices of UV-cured NOA65 (filled squares) and of two UV-cured mixtures of NOA65 and ROTN404: 20 volume percent LC (crosses) and 11 volume percent LC (diamonds). Also shown is the average refractive index of ROTN404 (pluses). The solid lines are fits to the data using Equations 3 and 4.

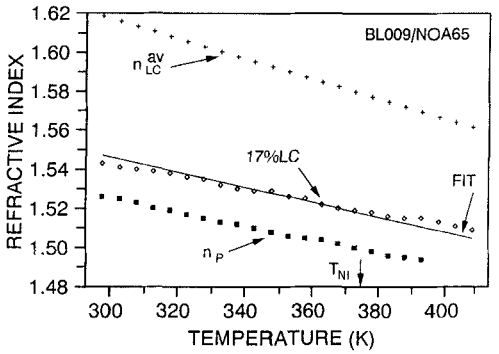

FIGURE 26 Temperature dependence of the refractive indices of UV-cured NOA65 (filled squares) and of a UV-cured mixture of NOA65 and 17 volume percent BL009 (diamonds). Also shown is the average refractive index of BL009 (pluses). The solid line is a fit to the data using Equations 3 and 4.

rule for this calculation has been previously shown to be valid for these mixed systems[13]:

$$n_{\text{mixture}} = xn_{\text{LC}}^{\text{av}} + (1 - x)n_p, \tag{4}$$

where x (= $X/100$) is the volume fraction of LC in the mixture, $n_{\text{LC}}^{\text{av}}$ is the isotropic average index for the LC and n_p is the polymer index. The isotropic average is given by

$$n_{\text{LC}}^{\text{av}} = (2n_0 + n_e)/3. \tag{5}$$

Since LC dissolved in the matrix is not birefringent, the use of the isotropic average index is proper. Indeed, Equation 5 is useful for temperatures both inside and outside the nematic range of the liquid crystal. For example, extrapolation into the isotropic range gives results in good agreement with measured indices.[13] As seen in Figures 25 and 26, Equation 5 accounts for the optical properties of the LCs at temperatures much higher than their individual T_{NI} values (indicated by arrows in Figures 25 and 26).

We now use $n_{\text{LC}}^{\text{av}}$ to model the refractive index of UV-cured mixtures in order to estimate solubility limits. As seen from Equation 3 and Figures 25 and 26, the refractive indices of the liquid crystals, the cured polymer, and the cured mixtures all vary linearly with temperature. Best fits to Equation 3 yield the fitting parameters shown in Table III. Three entries are given for each mixture: parameters determined from the measured indices (EXP); those calculated assuming additivity (Equation 4) (CALC); and those calculated from the model while allowing x to vary to give the best agreement with the data (FIT). These results show clearly that dn/dT is essentially the same for all cured mixtures and that, in each case, the fitted values agree well with experiment. Thus, we need only to focus on the differences between the fitted and measured values of the indices themselves.

As Figures 25 and 26 show,

$$n_{\text{LC}}^{\text{av}} > n_{\text{film}} > n_p, \tag{6}$$

TABLE III

Temperature dependence of the refractive index for two liquid crystals (ROTN404 and BL009), UV-cured NOA65, and selected UV-cured mixtures thereof[a]

Material or mixture	n_0	$(dn/dT)_{T0}$	X (vol. pct.)
ROTN404 (LC)	1.5928	−3.7353	
BL009 (LC)	1.6183	−5.1738	
NOA65 (polymer matrix)	1.5258	−3.4436	
11% ROTN404 in NOA65			
EXP	1.5298	−3.7740	
CALC	1.5332	−3.4757	11
FIT	1.5285	−3.4553	4
20% ROTN404 in NOA65			
EXP	1.5436	−3.5000	
CALC	1.5392	−3.5019	20
FIT	1.5436	−3.5209	26
17% BL009 in NOA65			
EXP	1.5433	−3.1130	
CALC	1.5415	−3.7377	17
FIT	1.5470	−4.0482	23

[a]Temperature range for evaluation of A: ~300 K to 400 K (~27°C to 127°C).

where n_{film} is the refractive index of the cured LC/polymer mixtures. This relationship results from two factors: 1) $n_e > n_0$ for all liquid crystals; 2) the index matching condition for optimum on-state PDLC film transparency requires that $n_0 = n_p$. Thus, from the definition of n_{LC}^{av} (Equation 3), one expects Equation 6 to be satisfied for all index-matched PDLC films. However, although the qualitative agreement between the data and the best-fit straight lines in Figures 25 and 26 is generally good, the values of the liquid crystal concentration, X, derived from the fitted curves do not agree well with the actual values at high LC concentrations (see Table III).

Index data and fitting parameters for cured ROTN404/NOA65 and BL009/NOA65 mixtures are shown in Figures 25 and 26 and Table III. Let us focus our attention on the former. For $X = 11\%$, the index of the cured mixture can be calculated from Equation 4 by assuming an effective LC concentration of $X = 4$ volume percent. Even though the actual LC concentration is 11%, the difference can be explained by taking into account the experimental error in the index (± 0.005). For example, if we take the index of NOA65 to be $n_p = 1.5208$ instead of 1.5258 (the value in Table III), we obtain good agreement between the LC concentration which best fits the data and the actual LC concentration.

For larger LC concentrations, the effect of n_{LC}^{av} on the matrix index increases, but agreement between the actual and fitted X values is still reasonable. However, when the solubility limit A is approached, the LC concentration ($X = 26\%$) which best fits the data becomes larger than the actual concentration ($X = 20\%$). Adjustment of n_p (within experimental error) can no longer yield agreement between actual and fitted X-values. Moreover, adjustment of the index of NOA65 to force a fit of the 11% data using $X = 4\%$ (as explained above), would require $X = 32\%$ for the best fit of Equation 4 to the data for $X = 20\%$. We attribute this fitting difficulty to two factors: 1) a change in degree of cure of the polymer with the addition of LC, and 2) the onset of optical non-linearities in the LC/polymer

mixtures[13] near their solubility limit. In the next section we will discuss these aspects in greater detail.

Although the previous methods enabled us to obtain estimated values for the solubility limit, it appears that the refractive index method, at best, sets only upper bounds on A. We arrive at this conclusion because we know of no fundamental reason for Equation 3 to break down at concentrations near the solubility limit. However, the RI method is still useful because of its simplicity and the fact that refractive index is routinely measured to optimize film performance.

From Figures 25 and 26 we estimate the upper bounds on the solubility limits for ROTN404/NOA605 and BL009/NOA65 mixtures to be 25 ± 5% and 20 ± 5%, respectively. Since index determinations were carried out over a wide temperature range the measurement temperature is taken to be 350 ± 50 K.

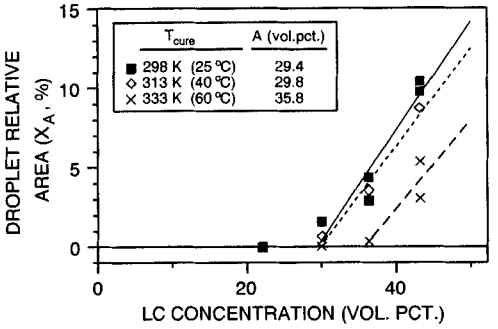

FIGURE 27 Droplet relative area, X_A; versus LC concentration, X, for PDLC films prepared at three different cure temperatures. The X-axis intercepts of the best fit lines give the corresponding A-values.

TABLE IV

Relative areas of droplets, X_a, and A-values for thermally-cured epoxy-based PDLCs (from SEM) (liquid crystal = MBBA/5CB [1:3][a])

Cure temperature	X (vol. pct.)	X_a (vol. pct.)	A (vol. pct.)
298 K (25°C)	30.0	1.6	29.4
	36.4	2.9	
	36.4	4.4	
	43.3	9.8	
	43.3	10.4	
313 K (40°C)	30.0	0.5	29.8
	36.4	3.4	
	43.3	8.7	
333 K (60°C)	36.4	0.3	35.8
	43.3	3.1	
	43.3	5.0	

[a]See text.
Note: temperature for evaluation of A: ~295 K (~22°C).

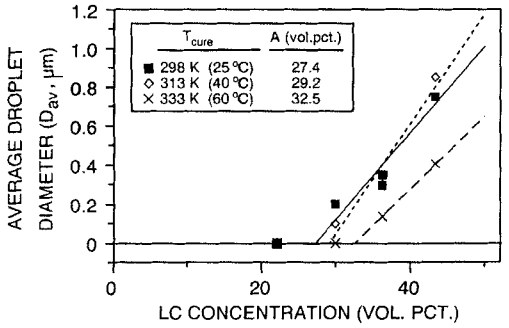

FIGURE 28 Average droplet diameters, D_{av}, versus LC concentration, X, for PDLC films prepared at three different cure temperatures. The X-axis intercepts of the best fit lines give the A-values.

TABLE V

Average droplet diameters, D_{av}, and A-values for thermally-cured epoxy-based PDLCs (from SEM) (liquid crystal = MBBA/5CB [1:3][a])

Cure temperature	X (vol. pct.)	D_{av} (μm)	A (vol. pct.)
298 K (25°C)	30.0	0.20	27.4
	36.4	0.30	
	36.4	0.35	
	43.3	0.75	
	43.3	0.75	
313 K (40°C)	30.0	0.10	29.2
	36.4	0.30	
	43.3	0.85	
333 K (60°C)	36.4	0.14	32.5
	43.3	0.40	
	43.3	0.40	

[a]See text.
Note: temperature for evaluation of A: ~295 K (~22°C).

Scanning Electron Microscopy

In our SEM studies we examined a single LC/polymer system. The liquid crystal was a 3:1 mixture (by volume) of 5CB and MBBA, where 5CB and MBBA are two single component liquid crystals, 4′-*n*-pentyl-4-cyanobiphenyl,[25] and *p*-methoxybenzylidene-p-n-butylaniline.[35] The polymer was Devcon 5-minute epoxy resin,[34] a two part system consisting of a diglycidyl ether from bisphenol A (Part A, 43 volume percent) and a mercaptan hardener (Part B, 57 volume percent). The 2-component liquid crystal and epoxy were stirred together at room temperature to produce mixtures containing 12.5, 22.2, 30.0, 36.4, and 43.3 volume percent liquid crystal. A small droplet of each mixture was then placed on top of an aluminum stud suitable for SEM studies and thermally cured at 298, 313, 333, 353, or 373 K (25, 40, 60, 80, or 100°C). Several SEM photomicrographs were recorded as described previously. The values of A reported are those corresponding to the temperature of sample metallization (slightly above room temperature) for a sample cured at a temperature T_{cure}.

From a collection of such SEM photos, we obtained the information needed to

TABLE VI

A-values (volume percent) for all PDLC Systems

Liq. Cryst.	Polymer	Cure Temp.	Meas. Temp.	*A*	Meas. Temp.	*A*
DSC results (thermal cure)						
5CB	Epoxy[a]	313 K	205 K	15.7	314 K	21.0
7CB	Epoxy[a]	313 K	205 K	10.3	317 K	15.4
E7	Epoxy[b]	323 K	215 K	16.0	336 K	8.1
E7	Epoxy[b]	343 K	215 K	12.9	336 K	10.5
E7	Epoxy[b]	363 K	215 K	15.4	336 K	16.8
ROTN404	Polyurethane	375 K	—	—	350 ± 25 K	15.5
ROTN404	Polyurethane	400 K	—	—	350 ± 25 K	16.8
DSC results (UV-cure)						
ROTN404	NOA65	300 K	225 K	18.6	367 K	37.5
ROTN404	NOA65	325 K	225 K	19.9	376 ± 5 K	35.9
ROTN404	NOA65	336 K	225 K	21.3	375 ± 5 K	27.7
ROTN404	NOA65	350 K	225 K	19.4	374 ± 5 K	40.9
ROTN404	NOA65	375 K	225 K	25.3	375 ± 5 K	41.6
BL009	NOA65	322 K	222 K	23.2	381 ± 3 K	42.3
BL009	NOA65	330 K	222 K	27.3	383 ± 3 K	44.3
BL009	NOA65	340 K	222 K	27.3	384 ± 5 K	45.8
BL009	NOA65	350 K	222 K	28.0	384 ± 5 K	44.3
BL009	NOA65	360 K	222 K	23.5	384 ± 5 K	46.3
BL009	NOA65	370 K	222 K	25.3	384 ± 5 K	47.9
BL009	NOA65	380 K	222 K	23.3	383 ± 5 K	52.5
TLS results (UV-cure)						
BL009	NOA65	~318 K	~295 K	~17		
BL009	NR1	~318 K	~295 K	~17		
BL009	P6008A	~318 K	~295 K	~17		
BL009	P6008B	~318 K	~295 K	~9		
RI results (UV-cure)						
ROTN404	NOA65	~318 K	350 ± 50 K	25 ± 5		
BL009	NOA65	~318 K	350 ± 50 K	20 ± 5		
SEM results (thermal cure)				from X_a		from D_a
5CB/MBBA (3:1)	Epoxy[c]	298 K	~310 K	29.4	~310 K	27.4
5CB/MBBA (3:1)	Epoxy[c]	313 K	~310 K	29.8	~310 K	29.2
5CB/MBBA (3:1)	Epoxy[c]	333 K	~310 K	35.8	~310 K	32.5

[a]2-part epoxy.[2,24]
[b]3-part epoxy.[2]
[c]5 minute epoxy.[34]

construct the phase diagram of Figure 3 from which qualitative solubility limits for each cure temperature can be obtained. The figure shows the range of cure temperatures and LC concentrations for which a microdroplet morphology was observed in the cured mixtures. Boxes containing the symbol "*N*" denote samples which did not exhibit microdroplets; boxes with a number indicate samples with LC droplets having a mean diameter, D_{av}, equal to that number (in μm). From the figure we see that the solubility limit of MBBA/5CB in epoxy increases for increasing cure temperature. For T_{cure} = 298 K (25°C) *A* is larger than ~22%; above $T_{cure} \simeq$ 353 K (80°C) all liquid crystal remains dissolved in the polymer matrix.

A quantitative determination of *A* as a function of cure temperature can be

obtained directly from the SEM photos. Even though the solubility limit is a volumetric quantity, the analysis can be made in terms of the relative area of the droplets in each sample which, of course, is obtainable from the SEM photos. We define the droplet relative area as:

$$X_a/100 = A_{\text{drop}}/A_{\text{SEM}}. \tag{7}$$

A_{drop} is the total area of all droplets, estimated from the number of droplets in the SEM photo and the corresponding average droplet diameter; A_{SEM} is the surface area of the film in the SEM. As shown previously[8,36,37] this relative area is approximately equal to the droplet relative volume:

$$X_a/100 = A_{\text{drop}}/A_{\text{SEM}} = V_{\text{drop}}/V_{\text{sample}}, \tag{8}$$

where V_{drop} is the volume occupied by all the droplets in a sample of volume V_{sample}. In Figure 27 are plotted values of X_a (determined from Equation 7 for three different cure temperatures) as a function of X. These plots allow us to estimate the solubility limit for that cure temperature from:

$$A = \lim_{X_a \to 0} X. \tag{9}$$

Since the data of Figure 27 are represented fairly well by a straight line, we can write:

$$X_a = (X - A)(dX_a/dX). \tag{10}$$

Fitting Equation 10 to the data of Figure 27 yields the A-values summarized in Table IV. As the cure temperature increases from 298 K to 333 K (25°C to 60°C) the solubility limit increases from 29.5% to 35.8%. An error of $\pm 0.5\%$ is associated with the least squares fit, but other errors, associated with the precision of determining droplet diameter and numbers, could result in a total error as large as 5% in A. (As can be seen from Figure 3, for $T_{\text{cure}} > 353$ K (80°C) all the LC is dissolved in the matrix.)

Finally, we point out that plots similar to those in Figure 27 can be constructed using D_{av}, the mean droplet diameter determined from each SEM micrograph. As seen in Figure 28, the dependence of D_{av} on LC concentration is approximately linear for the three cure temperatures. An estimate of solubility limits from these plots yields the A-values of Table V, which are in reasonable agreement with those from X_a. However, while a linear increase in X_a with X is intuitively reasonable, we know of no reason why this should be generally true for D_{av}. Indeed, although Smith[1] has previously observed a linear dependence of D_{av} on X for a polyurethane-based PDLC, the data of Golemme, *et al.*,[39] for an epoxy-based system exhibits an exponential behavior.[2]

SUMMARY

Although liquid crystal solubility in polymer-dispersed liquid crystals has been touched on previously,[3–5,40] a differential scanning calorimetry (DSC) method for measurement of the solubility limit for PDLCs, has only recently been demonstrated.[1,2,41] In this paper we have discussed the DSC technique and three additional methods (threshold for light scattering, refractive index, and scanning electron microscopy) for determining A and have presented results to illustrate all the methods. These results were acquired over a period of several years; as a result, no attempt was made to examine a single system by all four methods.

DSC has several advantages and a possible drawback. Its precision is greater than either TLS or RI. Although SEM appears to give comparably valid A-values, the temperature of the measurement is not well defined, whereas the DSC measurements are carried out in an environment where the temperature is precisely controlled. In addition, the existence of a theoretical model aids in the interpretation of the DSC results. The fact that DSC yields A-values for two temperatures (the LC glass transition and the nematic-isotropic transition) is of considerable value.[41] However, at least one of the other methods (TLS) can be adapted to measurements at more than one temperature. A drawback of DSC is the possibility that some components of a multi-component LC may preferentially dissolve in the polymer matrix. If this occurs, the measured values of both ΔC_{LC} and ΔH_{NI} would be affected, which in turn would alter the A-values. Such preferential dissolution may also affect the results of the other techniques. The problem of preferential solution may explain, in part, discrepancies between the methods.

As indicated above, SEM is, at present, apparently second to DSC in precision. However, TLS can probably be improved to a greater degree than SEM by carrying out the studies in a controlled temperature environment, using thermal microscopy. A-values for a range of temperatures could then presumably be obtained. TLS also has the advantage that it is the most rapid and convenient of the methods. Least successful of the techniques is probably RI since interpretation of the refractive index measurements requires the use of an incompletely validated model. Let us now discuss the results of these solubility limit studies.

Since solubility limits depend (inter alia) on PDLC constituents, cure temperature, and measurement temperature, it is worth while to summarize those parameters and the A-values for all the systems discussed in this report. This is done in Table VI. The first three columns identify the liquid crystal, the polymer matrix, and the cure temperature. Measurement temperatures and corresponding A-values are given in columns 4 and 5 and columns 6 and 7. In the case of the DSC results, the lower measurement temperature is for ΔC_{LC}, the higher one for ΔH_{NI}. For SEM, two types of analyses were carried out. The first set of A-values were derived from microdroplet relative areas; the second from droplet diameters.

It is useful to draw some conclusions from the Table. 1) From DSC measurements we see that the liquid crystal ROTN404 is much less soluble in polyurethane (thermally cured at 375 K) than in NOA65 (UV-cured at the same temperature). 2) A comparison of columns 5 and 7 shows that (as mentioned above) the DSC A-values for the two UV-cured systems are quite sensitive to measurement tem-

perature. The higher values determined at T_{NI} indicate that the liquid crystals are much more soluble at elevated temperatures. 3) The refractive index studies of the UV-cured ROTN404/NOA65 and BL009/NOA65 systems yield lower A-values (~25% and ~20%) than DSC (~36% and 42%) for comparable cure and measurement temperatures (~320 K and 350–380 K). It may be that RI, admittedly the least accurate of the methods, somewhat underestimates A. On the other hand, the TLS value for BL009/NOA65 (~17%) seems to agree with the RI result. However, it must be kept in mind that the TLS measurement was carried out at a lower temperature (~295 K), so that a value closer to the low-temperature DSC value (~23%) would be expected. Nevertheless, the possibility that DSC overestimates A must not be excluded. 4) The SEM study yields a slightly higher A-value (~28%) for 5CB/MBBA(3:1) LC in Devcon epoxy than that derived from DSC for pure 5CB in Bostik epoxy ($A \simeq 21\%$) for similar cure and measurement temperatures. Taking into account the differences in the liquid crystals and epoxies, the fact that the A-values from two such different methods are comparable in magnitude is reassuring.

The Table shows that A-values can take on a wide range of values depending on the PDLC components, their cure temperatures, and the measurement temperature. For the thermally cured systems, A-values range from 8 to 36 volume percent. For the UV-cured PDLCs, the range is broader: 9 to 53 volume percent. Obviously, care should be taken to discover liquid crystal/polymer combinations which give the greatest phase separation (lowest A-value) for efficient use of the LC.

Acknowledgments

The authors thank T. H. VanSteenkiste, D. B. Hayden, and W. D. Marion for technical assistance and G. P. Montgomery, Jr. for useful discussions.

References

1. G. W. Smith, *Mol. Cryst. Liq. Cryst.*, **180B**, 201 (1990).
2. G. W. Smith, G. M. Ventouris and J. L. West, *Mol. Cryst. Liq. Cryst.*, **213**, 11 (1992).
3. N. A. Vaz, G. W. Smith and G. P. Montgomery, Jr., *Mol. Cryst. Liq. Cryst.*, **146**, 1 (1987).
4. N. A. Vaz, G. W. Smith and G. P. Montgomery, Jr., *Mol. Cryst. Liq. Cryst.*, **146**, 17 (1987).
5. G. W. Smith and N. A. Vaz, *Liq. Cryst.*, **3**, 543 (1988).
6. G. P. Montgomery, Jr., N. A. Vaz and G. W. Smith, *Proc. SPIE*, **958**, 104 (1988).
7. N. A. Vaz, *Proc. SPIE*, **1080**, 2 (1989).
8. G. W. Smith, *Mol. Cryst. Liq. Cryst.*, **196**, 89 (1991).
9. Alufrit P-20, Atomergic Chemicals Corp., Farmingdale, NY.
10. Fusion Systems Co., Rockville, MD.
11. Non-uniform UV intensity has been shown to modulate the LC droplet microstructure. See, for example: A. M. Lackner, J. D. Margerum, E. Ramos and K. C. Lim, *Proc. SPIE*, **1080**, 53 (1989); J. H. Erdmann, A. M. Lackner, E. Sherman and J. D. Margerum, *SID Digest*, **22**, 602 (1991).
12. Fisher Scientific, Pittsburgh, PA.
13. N. A. Vaz and G. P. Montgomery, Jr., *J. Appl. Phys.*, **62**, 3161 (1987).
14. N. A. Vaz, G. W. Smith, G. P. Montgomery, Jr. and W. D. Marion, *Mol. Cryst. Liq. Cryst.*, **198**, 305 (1991).
15. International Scientific Instruments, Inc., Model SX-30.

16. Perkin-Elmer Corp., Norwalk, CT.
17. G. W. Smith, unpublished results.
18. S. Zumer and J. W. Doane, *Phys. Rev.*, **A34**, 3373 (1988).
19. G. P. Montgomery, Jr. and N. A. Vaz, *Phys. Rev.*, **A40**, 6580 (1989).
20. R. N. DeMartino, G. H. Khanarian, T. M. Leslie, M. J. Sansone, J. B. Stamatoff and H. N. Yoon, *Proc. SPIE*, **1105**, 2 (1989).
21. J. W. Doane, J. L. West, W. Tamura-Lis and J. B. Whitehead, Jr., *Proc. First Pacific Polymer Conference*, Maui, Hawaii, Dec. 12–15, 1989, p. 245.
22. J. W. Doane and J. L. West, European Patent Applic. WO 89/09807, Oct. 19, 1989. J. W. Doane and J. L. West, *SID Digest*, **21**, 224 (1990).
23. G. M. Ventouris and J. L. West, private communication.
24. Bostik Division of Emhart Corp., Middleton, MA.
25. Merck Ltd., Poole, England.
26. F. Hoffman-LaRoche & Co., Ltd., Basle, Switzerland.
27. Norland Products, Inc., North Brunswick, NJ.
28. N. A. Vaz and G. W. Smith, U.S. Patent 4, 728,547, 1 March 1988.
29. F. G. Yamagishi, L. J. Miller and C. I. van Ast, *Proc. SPIE*, **1080**, 24 (1989).
30. N. A. Vaz, *Proc. SPIE*, **1080**, 2 (1989).
31. The NR1 formulation contains NOA65 and a photosensitizer to broaden the range of wavelengths useful in the cure process.
32. P6008A contains Photomer 6008, a diurethane diacrylate from Diamond Shamrock, Morristown, NJ, pentaerithritol-tekrakis-(3-mercaptopropionate) from Polysciences, Inc., Warrington, PA, and the photoinitiator Darocure 1173 from Merck Ltd., Poole, England.
33. P6008B is similar to P6008A, but with an additional accelerator, N,N-dimethylaminoethanol from Aldrich Chemical Co., Milwaukee, WI.
34. Devcon Corp., Danvers, MA.
35. Eastman Organic Chemicals, Rochester, NY.
36. R. L. Fullman, *Trans. AIME*, **197**, 447 (1953).
37. N. A. Vaz, unpublished results (see reference 11 cited in reference 8).
38. J. L. West, *Mol. Cryst. Liq. Cryst.*, **157**, 427 (1988).
39. A. Golemme, S. Zumer, D. W. Allender and J. W. Doane, *Phys. Rev. Lett.*, **61**, 2937 (1988).
40. T. Kajiyama, S. Washizu and M. Takayanagi, *J. Appl. Polym. Sci.*, **29**, 3955 (1984); A. Miyamoto, H. Kikuchi, Y. Morimura and T. Kajiyama, *New Polymeric Mater.*, **2**, 27 (1990).
41. G. W. Smith, *Mol. Cryst. Liq. Cryst.*, **225**, 113 (1993).